Polymer Chemistry

Accepted Manuscript

Journal Name

ARTICLE

The influence of surface grafting on the growth rate of polymer chains

Received 00th January 20xx,
Accepted 00th January 20xx

DOI: 10.1039/x0xx00000x

www.rsc.org/

Chengjun Kang, [a] Rowena Crockett, [b] and Nicholas D. Spencer *,[a]

The effect of surface grafting on growth kinetics during controlled radical polymerization (CRP) was investigated by comparing the growth of polymers in solution with that on a flat silicon surface. The surface-grafted polymers were attached to the surface via a photo-cleavable initiator, which allowed the polymers to be detached by means of UV light with a wavelength that did not lead to polymer photolysis. The molecular weights of surface- and solution-grown polymers were determined by size-exclusion chromatography (SEC). It could be shown that for a series of polymers synthesized from alkyl methacrylate monomers, it was principally the grafting density that determined the ratio of the molecular weight on the surface to that in solution.

Introduction

Controlled Radical Polymerization (CRP) has been extensively applied in a wide variety of fields in recent years[1], due to its simplicity and many practical advantages. CRP can be conveniently carried out in solution, to generate polymers with narrow polydispersity index (PDI), and also can be initiated from surfaces to grow densely tethered polymer brushes[2] from a wide variety of monomers.

Since the determination of the molecular weight of surface-grafted polymers is challenging, solution polymerization has often been carried out in parallel, with the aim of characterizing the solution-generated polymers under the assumption that they resemble those grown on the surface. For this reason, it is of great interest to determine the relationship between the molecular weight of polymers grown on the surface and in solution, and this has been the subject of a number of studies. In many cases, polymer brushes were grown from nanoparticles, which provide sufficient quantities of polymers for analysis, thanks to their large surface area[1b, 2c, 3]. It was observed that polystyrene (PS) grown on silica nanoparticles using nitroxide-mediated polymerization resulted in a higher molecular weight of surface-grafted polymers (51 kDa) than those generated in parallel in solution (48 kDa)[4]. In that study, polymers were grafted to the surface via cleavable ether linkages that could be broken with an excess of trimethylsilyl iodide[4]. The larger molecular weight of the surface-grafted polymers was attributed to the curvature of the silica particles, which would alleviate any possible steric effects at the reaction site[4]. Polymerizations of styrene and methyl methacrylate (MMA) have also been carried out on silica particles using atom-transfer radical polymerization (ATRP). Passeto et al. found higher molecular weights for the PS and poly(methyl methacrylate) (PMMA) in solution than for the surface counterparts[5]. The author attributed the difference in chain length to the termination of polymerization in mesopores of the silica[5]—a process that would not be expected on a flat surface. It has also been shown that the molecular weight of PMMA grown from silica nanoparticles is dependent on the sizes of particles when their diameters are below 130 nm[6]. In another study, PS was grown from a polymer substrate by ATRP via initiators that could be cleaved in strong acid, such as p-toluenesulfonic acid/dioxane solution[7]. In that investigation, the molecular weight of the cleaved polymer brush was found (in most cases) to be significantly larger than that of the polymer generated in solution.

CRP has also been numerically simulated, both on planar substrates and in solution, assuming that side-reactions were absent[8]. The simulation results showed the surface-initiated polymerization proceeds more slowly and with a higher polydispersity index (PDI) than polymerization taking place in solution. The authors attributed these differences to the much more crowded environment of the active chain ends (where growing polymer, monomer, catalyst, and ligand all interact) in surface-tethered polymers, compared to their counterparts in solution. Their simulation results were further tested experimentally, PMMA brushes being grown from flat silica surfaces, and subsequently degrafted using tetrabutylammonium fluoride[9]. The dependence of grafting density on Cu^{II}/Cu^{I} ratio was investigated, and the authors found that higher ratios led to better controllability, with the

[a.] Laboratory for Surface Science and Technology, Department of Materials, ETH Zurich, Vladimir-Prelog-Weg 5, 8093 Zurich, Switzerland.
[b.] Swiss Federal Laboratories for Materials Science and Technology, Empa, Ueberlandstrasse 129, CH 8600 Dübendorf, Switzerland.
[c.] E-mail: nspencer@ethz.ch (N.D.Spencer).

† Electronic Supplementary Information (ESI) available. See DOI: 10.1039/x0xx00000x

formation of denser PMMA brushes[9b]. It was concluded that the growth of polymer chains in highly crowded environments was the major cause of chain termination, since it led to a deviation from "living" polymerization.

In a previous study[10], we showed that polymer brushes could be detached from planar substrates by the introduction of a photo-cleavable group, the 2-nitrobenzyl moiety, into a surface-initiated atom-transfer radical polymerization (SI-ATRP) initiator. Following surface polymerization, surface attached polymer chains could be efficiently cleaved under 254-nm-UV illumination. A disadvantage of that approach was that 254 nm UV can also photolyze the polymer to a certain extent, thereby compromising the precise measurement of $Mn_{surface}$ and $PDI_{surface}$. To circumvent this problem, in the present study, a photo-cleavable SI-ATRP initiator has been synthesized (**7**, Scheme 1), and this can be cleaved at 366 nm. This initiator has been used to grow polymers from flat silicon surfaces from a broad range of methacrylate monomers, as well as methyl acrylate and styrene, for comparison. Following the photochemical detachment of grafted polymers, the released polymers were characterized by SEC and the results compared to those of polymers grown in parallel in solution. The influences of monomer, free-initiator concentration, polymerization temperature, and grafting density of polymer brushes have been examined.

Experimental details

Materials

Monomers were purchased from Sigma Aldrich AG (Switzerland) and inhibitors were removed from all monomers by passing them through a basic alumina column. CuBr (Sigma Aldrich AG, Switzerland) was purified by firstly washing with acetic acid and subsequently with acetone, then it was dried under vacuum and stored under argon. All other reagents that were commercially available were used as received. If not specified otherwise, all solvents were reagent grade and used without further purification.

Instrumentation

The chemical structures of all products were determined with ^{1}H NMR and ^{13}C NMR (Bruker Avance 300 spectrometer (Bruker, Germany)). FT-IR spectra of all compounds were recorded by a Bruker infrared spectrometer (IFS 66, Bruker, Germany). The UV-vis spectrum of the photo-cleavable initiator was recorded by a V-600 spectrometer (JASCO, Japan), with a measurement range of 400-700 nm and a scanning speed of 100 nm/min. The thicknesses of dry organic layers on silicon substrates were measured by a variable-angle spectroscopic ellipsometer (VASE, M-2000F, LOT Oriel GmbH, Darmstadt, Germany) at an incident angle of 70°. A three-layer model was used and each sample measured three times at three different locations[11]. The molecular weights of all polymers were measured by a Viscotek Size-Exclusion Chromatography (SEC)-system, equipped with a pump, a degasser (SEC max VE2001), a detector module (Viscotek 302 TDA), a UV detector (Viscotek 2500, λ=254nm), a refractive-index (RI) detector and two columns (PLGel Mix-B, PLGel Mix-C), using chloroform as eluent with a flow rate of 1.0ml/min. The molecular weights of all polymers were calibrated by the universal calibration method, with polystyrene standards in the range of Mp 1 480 to 4 340 000 Da.

Synthesis of photo-cleavable SI-ATRP initiator (7)

*Synthesis of 2-((2-bromo-2-methylpropanoyl)oxy)ethyl 4-(4-acetyl-2-methoxy-5-nitrophenoxy)butanoate (**5**).*

Compound **1** is commercially available, compounds **2** to **4** were synthesized according to a previously described method[12]. The typical procedure for the synthesis of **5** is as follows: compound **4** (0.8 g, 2.7 mmol), N,N-dicyclohexylcarbodiimide (DCC) (0.8g, 3.9 mmol), and 4-dimethylaminopyridine (DMAP) (39.0mg, 0.32mmol) were dissolved in 20 ml anhydrous THF, and then 2-hydroxyethyl 2-bromo-2-methylpropanoate[13] (0.58 g, 2.7 mmol) in 0.5 ml anhydrous THF was added. After stirring for 24 h, the precipitate was filtered and the solvent removed under vacuum, the obtained crude product being dissolved in ethyl acetate (EtOAc), then washed by HCl-acidified brine solution (pH ≈ 2.0), dried by anhydrous $MgSO_4$, and finally evaporated to yield a brown viscous oil. Chromatography on silica gel (ethyl acetate: hexane= 1: 1) afforded compound **5** (1.2g, 90% yield) as a light-brown, viscous oil. ^{1}H NMR (See Supplementary Information for spectrum, Figure S2) (300MHz, *d*-$CDCl_3$(δ 7.20)): δ (ppm) 7.54 (s, 1H), 6.68 (s, 1H), 4.31 (m. 4H), 4.09 (t, 2H), 3.89 (s, 3H), 2.52 (t, 2H), 2.43 (s, 3H), 2.14 (quint, 2H), 1.86 (s, 6H). ^{13}C NMR (300 MHz, *d*-$CDCl_3$(δ 77.05)): δ (ppm) 200.02, 172.49, 171.47, 154.31, 148.45, 138.40, 132.91, 108.81, 108.07, 68.38, 63.49, 61.88, 56.61, 55.41, 30.67, 30.39, 24.12, 24.03. IR (cm^{-1}): 2951.6, 1738.3, 1712.9, 1515.3, 1220.6, 1153.6.

Synthesis of 2-((2-bromo-2-methylpropanoyl)oxy)ethyl 4-(4-(1-hydroxyethyl)-2-methoxy-5-nitrophenoxy)butanoate (**6**).

To a solution of **5** (2.80 g, 5.7 mmol) in 140 ml MeOH at 0 °C, $NaBH_4$ (0.12 g, 3.1 mmol) was added under gentle stirring. A small amount of gas was generated and the mixture was allowed to react for 20 min. Reduction of the ester bond by $NaBH_4$ is observed if the reaction is carried out at room temperature. The reaction was terminated by the addition of 100 ml sat. NH_4Cl (aq) and the mixture was extracted by EtOAc, the organic phase being dried by anhydrous $MgSO_4$ and evaporated. The crude product was further purified by passing it through a silica-gel column with hexane and EtOAc (v/v= 1:1) as eluent, to yield a light-brown, viscous oil (1.4 g, 56% yield). ^{1}H NMR (See Supplementary Information for spectrum, Fig. S2) (300 MHz, *d*-$CDCl_3$(δ 7.20)): δ (ppm) 7.50 (s, 1H), 7.23 (s, 1H), 5.49 (quint. 1H), 4.31 (m, 4H), 4.05 (t, 2H), 3.91 (s, 3H), 2.52 (t, 2H), 2.18 (d, 1H), 2.13 (quint, 2H), 1.85 (s, 6H). 1.48 (d, 3H). ^{13}C NMR (300 MHz, *d*-$CDCl_3$(δ 77.04)): δ (ppm) 172.62, 171.49, 154.14, 146.92, 139.58, 136.98, 109.15, 108.76, 68.20, 65.79, 63.52, 61.82, 56.36, 55.39, 30.67, 30.46, 24.30, 24.23. IR (cm^{-1}): 2973.6 1744.1, 1525.6, 1263.8,1159.4.

Synthesis of 2-((2-bromo-2-methylpropanoyl)oxy)ethyl 4-(4-(1-((((2,5-dioxopyrrolidin-1 yl)oxy)carbonyl)oxy)ethyl)-2-methoxy-5-nitrophenoxy)butanate **(7).**

0.51 g (2.0 mmol) N,N'-disuccinimidyl carbonate was added to a mixture of **6** (0.25 g, 0.5 mmol) and DMAP (33 mg, 0.27 mmol) in 10 ml anhydrous CH_3CN, the mixture being stirred for 24 h in darkness at 40°C. If not specified otherwise, all experiments described below were carried out under the exclusion of light. The completion of the reaction was determined by a single peak being visible in thin-layer chromatography (TLC), with hexane/ EtOAc (50%/ 50%) as mobile phase. Then the solvent was evaporated and the obtained semi-solid was purified by chromatography on silica gel (ethyl acetate: hexane= 1: 1). This yielded compound **7** (0.50g, 76% yield) as a light brown semi-solid. ^{1}H NMR (See Supplementary Information for spectrum, Fig. S2) (300 MHz, *d*-$CDCl_3$(δ 7.19)): δ (ppm) 7.57 (s, 1H), 6.99 (s, 1H), 6.42 (q. 1H), 4.31 (m, 4H), 4.06 (t, 2H), 3.97 (s, 3H), 2.73 (s, 4H), 2.52 (t, 2H), 2.13 (quint, 2H), 1.85 (s, 6H). 1.68 (d, 3H), ^{13}C NMR (300 MHz, *d*-$CDCl_3$(δ 77.04)): δ (ppm) 172.59, 171.49, 168.45, 154.63, 150.59, 147.67, 139.20, 131.26, 109.17, 107.36, 68.18, 63.53, 61.84, 56.52, 55.42, 30.66, 30.43, 25.44, 24.18, 21.96. IR (cm^{-1}): 2962.0, 1819.2, 1789.2, 1738.3, 1519.9, 1216.0, 1080.8.

Fabrication of photo-cleavable-SI-ATRP-initiator-modified silicon substrates

Si(100) wafers were cut into 2.5× 4.0 cm^2 pieces, which were cleaned by sonication in 2-propanol for 3 × 10 min, prior to being oxidized in a UV/ozone chamber for 30 min. In order to immobilize **7** onto silicon-wafer surfaces, the silicon substrates were first functionalized with amino groups by coating with (3-aminopropyl) triethoxysilane (APTES) via vapor-phase deposition[10]. The immobilization of **7** onto APTES-modified silicon substrates is achieved by immersing freshly prepared APTES-modified silicon substrates into an anhydrous THF solution of **7** at a concentration of 10 mg/ml, without stirring. The amount of initiator immobilized on the substrates can be adjusted by controlling the immersion time of substrates in THF solution. After various lengths of time (from 5h to 24h), the wafers were removed from solution and briefly sonicated in THF, before being finally dried in a nitrogen stream. The successful immobilization of **7** onto APTES-modified substrates was demonstrated both by the direct observation of amide-bond formation at 1665 cm^{-1} in the multiple-transmission-reflection infrared spectrum (MTR-IR)[14], and an increase in the organic layer thickness of about 1.5 nm—the calculated height of the initiator when fully extended from the aminated surface is approximately 1.8 nm, and thus 1.5 nm corresponds to an estimated 83 % of a monolayer coverage.

Polymerization

The methods used in this study for the polymerization of dodecyl (lauryl) methacrylate[10], butyl methacrylate[15], methyl methacrylate[3b], methyl acrylate[16] and styrene[16] in a controlled manner have been adapted from those reported in previous publications. The polymerization procedures are similar for all monomers (Table 1). A representative example is as follows: 0.164 g (0.4 mmol) 4,4’-dinonyl-2,2’-bipyridyl (dNbpy) was dissolved in 35 ml (0.33 mol) of methyl methacrylate, the mixture undergoing four freeze-pump-thaw circles (15 min each) to remove dissolved oxygen. Then the mixture was transferred to another flask containing 26.8 mg CuBr (0.187 mmol) and 4.4 mg $CuBr_2$ (0.019 mmol). After stirring for 10 min at 100 °C, 5 ml methyl methacrylate, with 24.0 mg (0.048 mmol) compound **5** dissolved as a free initiator, was added to the mixture, which was immediately transferred to freshly prepared, initiator-modified silicon substrates. Polymerization was carried out at 100 °C for various lengths of time without stirring, after which the silicon substrates were removed from the polymerization solution, sonicated in chloroform and then underwent Soxhlet extraction for 24h to remove weakly adsorbed polymer. Polymer generated by the free initiator was collected by precipitating the polymerization solution in MeOH as soon as the silicon substrates had been removed from the flask. The precipitate was collected, redissolved in CH_2Cl_2 and precipitated in MeOH, this process being repeated several times until the precipitate was free of blue color, and then it was dried under vacuum. Detailed information concerning polymerization conditions for each monomer has been included in Table 1.

Table 1 Polymerization conditions for each monomer.

M	L	[M]: [I]: L: CuBr: $CuBr_2$	T (°C)	Solvent	t (h)
LMA	dNbpy [a]	2000:1:2.1:1:0.05	100	bulk	15
BMA	dNbpy	2000:1:11:5:0.5	25	45%isopropanol/5%H_2O	5
tert-BMA	dNbpy	2000:1:11:5:0.5	25	45%isopropanol/5%H_2O	17
MMA	dNbpy	2000:0.25:2.2:1:0.1	90	bulk	1.2
MA	PMDETA [b]	2000:0.4:5.3:5:0.15	70	bulk	7
Styrene	PMDETA	2000:0.5:6.2:6:0.18	100	bulk	6.5

M: Monomer; L: Ligand; I : initiator; T: Temperature; t : Polymerization time.

[a] 4, 4’-Dinonyl-2, 2’-bipyridyl,

[b] N,N,N′,N′,N′′-pentamethyldiethylenetriamine

Cleavage, harvesting, and characterization of polymer brushes on silicon substrates

Following Soxhlet extraction, the freshly cleaned, polymer-brush-modified silicon substrates were transferred to a cleaned glass dish, and polymer brushes were cleaved off by exposing the sample to UV light (366 nm) with a power density of 2.8 mW/cm^2 for 1h in a dry state, after which about 90% reduction in thickness was observed for all polymers. In order to gather the cleaved polymer, the illuminated substrate was washed 3 times (1 ml each) with chloroform, the washings being combined and transferred to a dust-free flask, after

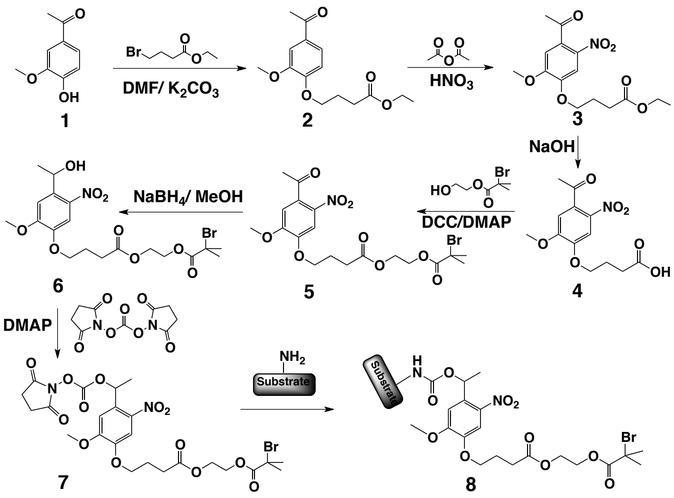

Scheme 1. Synthesis of the photo-cleavable SI-ATRP initiator.

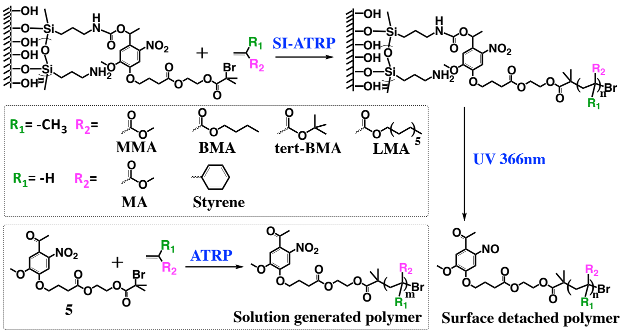

Scheme 2. Polymerization reactions, both on surface and in solution.

which the chloroform was removed under vacuum, the cleaved polymer being clearly observed at the bottom of the flask. It was subsequently dissolved in 240 μl chloroform for SEC measurement. The UV-detector signal intensity during SEC measurements provided evidence that the detached polymer chain was connected to an aromatic ring (part of the photo-labile linker), indicating that the polymers had been cleaved from the surface through the breakage of photo-labile moieties (see Supporting Information Figure S5).

Results and discussion

Growth and detachment of polymer brushes from planar substrates

The photo-cleavable SI-ATRP initiator used to generate grafted polymer brushes was synthesized (**7**, Scheme 1) by introducing two alkoxy groups into the 2-nitrobenzyl moiety[17], which places the activation wavelength of the photophore significantly above 300 nm, which does not induce photolysis of the polymer chains (see Supporting Information). The photo-cleavable SI-ATRP initiator **7** was synthesized via a six-step procedure (Scheme 1).

Initiator-modified substrates, **8** could be fabricated through the reaction between the active ester group of **7** and the amino group of (3-aminopropyl) triethoxysilane (APTES)-modified silicon substrates[10]. The molecular weights and PDIs of polymers that were simultaneously generated both on lanar substrates (Mn_{surf}, PDI_{surf}) and in bulk solution (Mn_{sol}, PDI_{sol}) in the same polymerization system were determined for six different monomers: dodecyl (lauryl) methacrylate (LMA), *n*-butyl methacrylate (BMA), *tert*-butyl methacrylate (*tert*-BMA), methyl methacrylate (MMA), methyl acrylate (MA) and styrene (S) (Scheme 2).

The first four methacrylate monomers contain side groups differing in chain lengths or branching, thus allowing the influence of steric differences on the polymerization process to be examined. The monomer set investigated also includes MA, as a representative of acrylate monomers, and styrene as an example of aromatic monomer. The overall polymerization reactions are shown in Scheme 2. In order to minimize the difference between the initiator adsorbed on the substrate and the free initiator in solution, compound **5** was used as the free initiator.

Surface-tethered polymers were detached by exposing the dried, polymer-brush-covered substrates to 366 nm UV radiation. No detectable decomposition of the polymer chains occurred under these conditions (Supporting Information, Figure S3). The detached polymer chains were harvested by washing the illuminated substrates with chloroform, the solvent being subsequently removed under vacuum. All polymers were analyzed by means of SEC. The concentration of detached polymer obtained for SEC measurement was less than 1 mg/ml due to the minimal amount of polymer generated on planar substrates. Nevertheless, the polymer signals from the refractive index (RI) detector showed high S/N ratio (see Supporting Information). Each experiment was repeated three times (see Supplementary Information Tables S1 and S2), resulting in collective errors from the beginning of the polymerization to the SEC measurement. The variation in ellipsometry measurements of dry thickness within each set of measurements indicates that the largest contributor to the error was the variability in the polymerization process itself, rather than in subsequent SEC measurements.

Influence of grafting density on the difference between surface-grafted and solution-phase polymerization

The grafting density of the surface-tethered polymer brushes was calculated from the dry thickness, the measured average molecular weight (Mn) of surface-grafted polymer, and the bulk density[7,18] of polymers. The ratio of Mn_{sol}/ Mn_{surf} versus grafting density for the alkyl methacrylates, methyl acrylate and styrene is shown in Figure 1, from which we can see that higher grafting densities correspond to higher Mn_{sol}/Mn_{surf} ratios. Patil et al. found in their modeling study that the grafting density of PMMA was influenced by the molar ratio

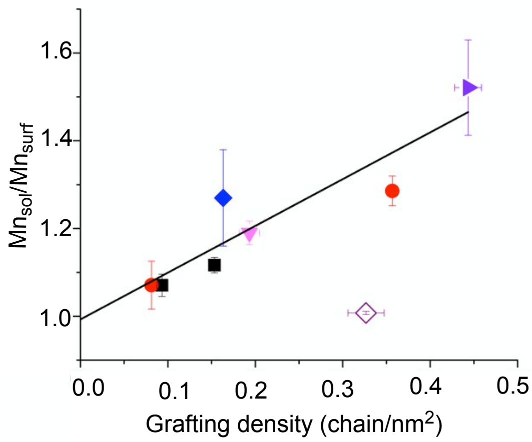

Figure 1. Ratio of the molecular weight of polymers generated in solution and those simultaneously produced on the surface: ● PMMA at two different grafting densities ■ PLMA at two different grafting densities, ▼ P-t-BMA, ▶ PMA, ◆ PBMA and ◇ polystyrene. The line is intended only as a guide to the eye, and was calculated using the measurements for polyacrylate, polymethacrylates as well as a ratio (Mn_{sol}/Mn_{surf}) of 1 at a grafting density of 0. The measurement for polystyrene was not used in the calculation.

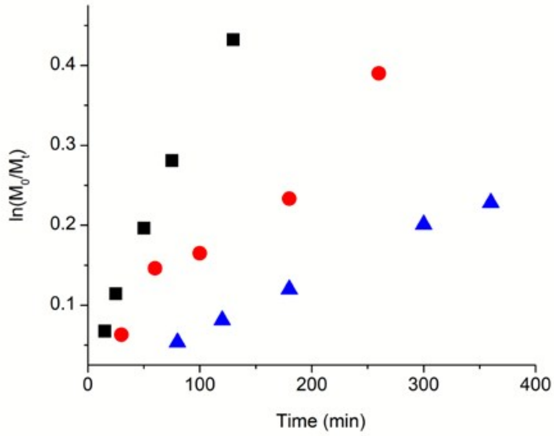

Figure 2. Conversion of MMA with time under polymerization conditions, at 90 °C with high (1.2 mM, ■) and low (0.59 mM, ●) free initiator concentrations, and at 60 °C with low (0.59 mM, ▲) initiator concentration. M_0 is the initial monomer concentration and M_t is the monomer concentration at time t. The solution and surface polymers were formed in the same monomer solution in each experiment, however, as the quantity of surface polymer is negligible in comparison to the quantity of solution polymer, this conversion can be interpreted as describing the reaction to form solution polymer.

between deactivator (Cu^{II}/Ligand) and catalyst (Cu^{I}/Ligand), due to the steric crowding at the reaction site[9]. It is therefore possible that the structure of the monomer influences the Mn_{sol}/Mn_{surf} ratio by altering the grafting density of polymer brushes, leading to the appearance of a relationship between the two. In line with the findings of Patil et al, the bulkier LMA leads to a polymer with a lower grafting density than the much smaller methyl acrylate. This trend was investigated more closely for LMA and MMA. The Cu^{II}/Cu^{I} was kept constant in all experiments and the grafting density controlled by varying the time allowed for the reaction of initiator **7** with the APTES-modified silicon substrates. It can be seen in Figure 1 that the Mn_{sol}/Mn_{surf} ratio for both PLMA (squares) and PMMA (circles) was lower at lower grafting density. These measurements of polyacrylates and polymethacrylates indicate that it is not the size or the structure of the monomer themselves that are playing a role in determining the ratio of molecular weights in solution and at the surface, but rather the consequent grafting densities.

The observation that higher grafting density and thus greater crowding of polymer brushes leads to higher Mn_{sol}/Mn_{surf} ratios could be explained in two ways: firstly, greater crowding could lead to the growing polymer chain ends being more readily terminated. This effect would result in both a higher PDI value and lower average molecular weight for surface-grafted polymer chains. A second possibility is that the crowding of polymer chains hinders the delivery of reactants to the reactive chain ends, thus reducing the propagation rate of surface-tethered polymer chains. Both explanations would imply that polymer brushes with extremely low grafting densities would share the same polymerization behavior as their solution-phase counterparts. This is indeed borne out by extrapolating the results in Figure 1 to the limit of negligible grafting density. In this case the Mn of surface-bound chains appears to be the same as that of polymer chains synthesized in the solution (i.e. Mn_{sol}/Mn_{surf} = 1). In addition, a number of studies involving Mn measurements of polymers cleaved from nanoparticles have led to the conclusion that the surface-grafted and solution-generated polymers do not have significantly different molecular weights[19]. It seems likely that this observation is either due to a low grafting density or the influence of the curvature of the nanoparticles, which allows the polymer chain-ends to be further apart, effectively behaving as if the grafting density were low.

Influence of free initiator concentration, conversion, and polymerization temperature on the difference between surface-grafted and solution-phase polymerization

A kinetic study was carried out with MMA to determine the factors that may contribute to differences between the rates of polymerization on the surface and in solution. The rate of polymerization for ATRP is given by[20]:

$$\mathrm{R} = k_p K_{eq} [\mathrm{I}] \frac{[\mathrm{CuBr}]}{[\mathrm{CuBr_2}]} [\mathrm{M}]$$

Where k_p is the rate constant for propagation, K_{eq} is the ratio between the rate constants for activation and deactivation, and [I] and [M] are the concentrations of initiator and monomer, respectively. Polymerization reactions were carried out simultaneously in solution and on the surface, with MMA

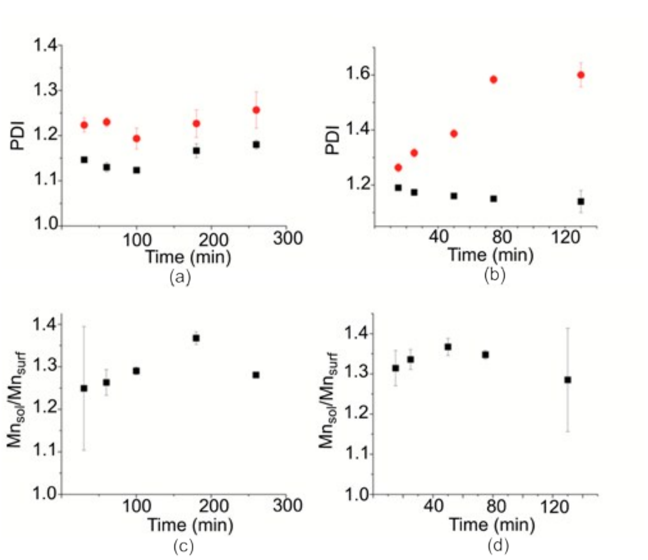

Figure 3. PDI values for PMMA generated in solution (■) and on the surface (●) for (a) an initiator concentration of 0.59 mM at a reaction temperature of 90 °C, and (b) at an initiator concentration of 1.2 mM at 90 °C. (c) Mn$_{sol}$/Mn$_{surf}$ ratio for PMMA at an initiator concentration of 0.59 mM at 90 °C and (d) at an initiator concentration of 1.2 mM at 90 °C.

as the monomer, at different temperatures and concentrations of free initiator in solution. The consumption of monomer with time for initiator concentrations in solution of 1.2 mM or 0.59 mM at 90 °C, as well as an initiator concentration of 0.59 mM at 60 °C are shown in Figure 2.

The slope for the consumption of monomer in solution shown in Figure 2 at an initiator concentration of 1.2 mM is approximately twice that for the consumption of monomer at an initiator concentration of 0.59 mM. The higher initiator concentration increased the rate of reaction in solution by increasing the number of propagating chains. The molecular weight of the chains in solution and thus the ratio Mn$_{sol}$/Mn$_{surf}$ did not vary significantly with increasing initiator concentration (Figs. 3c and 3d).

Furthermore, the relationship between grafting density and the Mn$_{sol}$/Mn$_{surf}$ ratio was not influenced significantly by increasing the concentration of free initiator. The average grafting density for the experiments carried out with initiator concentration at 0.59 mM was 0.33 ± 0.02 chains nm^{-2} with Mn$_{sol}$/Mn$_{surf}$ being 1.29 ± 0.05, and as for the initiator concentration of 1.2 mM, the grafting density was 0.30 ± 0.02 chains nm^{-2} with Mn$_{sol}$/Mn$_{surf}$ being 1.33 ± 0.03. Increasing the initiator concentration did have a significant effect on the relative values of PDI (Figs 3a and b), however. At low initiator concentration, the PDI remained constant over time, within the experimental error, with a slightly lower value for the polymer formed in solution than for the PMMA grafted from the surfaces (Figure 3a). On the other hand, at high free initiator concentration, the PDI of the PMMA formed at the

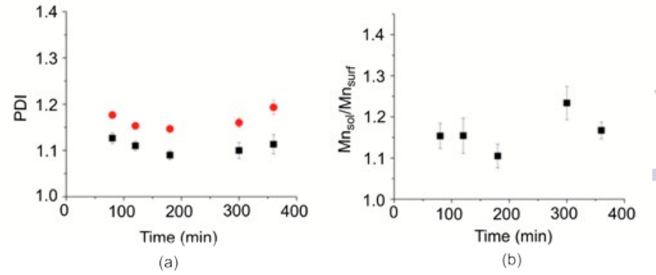

Figure 4. (a) PDI versus time for the polymerization of MMA at 60 °C and an initiator concentration of 0.59 mM ■ in solution and ● on the surface. (b) Mn$_{sol}$/Mn$_{surf}$ ratio for the polymerization of methyl methacrylate at 60 °C and an initiator concentration of 0.59 mM.

surface increased with time, indicating a decrease in the controlled nature of the polymerization at the surface (Figure 3b), possibly due to the larger number of solution-based growing chains. However, the high PDI values of PMMA on the surface did not have a significant effect on the Mn$_{sol}$/Mn$_{surf}$ ratio (Figure 3d). It should be noted that the errors associated with each measurement of Mn and PDI result from the entire polymerization procedure—from the amination of the silicon surface and production of monomer solution to the measurement of molecular weight—and are not due to the resolution of the SEC instrument.

At lower polymerization temperature (60 °C), PDI values for both surface- and solution-generated polymers were slightly lower than those of polymers generated at 90 °C, and a significant decrease in the Mn$_{sol}$/Mn$_{surf,}$ ratio to an average value of 1.16 ± 0.05 was observed (Figure 4). The rate of propagation is strongly influenced by the temperature and the rate coefficient (k_p) is given by the Arrhenius equation[21].

The value of k_p for PMMA at 90 °C is 1602 L mol^{-1}s^{-1} and at 60 °C is 821 L mol^{-1}s^{-1} [21], and therefore, the relative rate of reaction would be 0.51, if it were only the rate of propagation that is influenced by temperature ($k_{p60°C}/k_{p90°C}$). The ratio of the slopes for ln(M_o/M_t) versus time at the two polymerization temperatures (with the same initiator concentration) was very close to this value, at 0.50 (Figure 2). It can therefore be concluded that, upon decreasing temperature, the rate of reaction in solution decreases in line with the expected decrease in the rate of propagation, but the rate of reaction on the surface decreases to a lesser extent. Thus, at lower temperatures, the molecular weights of polymer on the surface and in solution become more similar.

Styrene was also polymerized from the silicon surface via ATRP to determine the influence of monomer chemistry on the ratio Mn$_{sol}$/Mn$_{surf}$. This measurement is shown along with those of the methacrylates in Figure 1. The Mn$_{sol}$/ Mn$_{surf}$ ratio for polystyrene clearly deviates from the trend followed by the methacrylates and methyl acrylate, with a value of 1.01 ± 0.01 at a grafting density of 0.33 ± 0.02 chain/nm^2. The rate coefficient for propagation (k_p), however is relatively low at

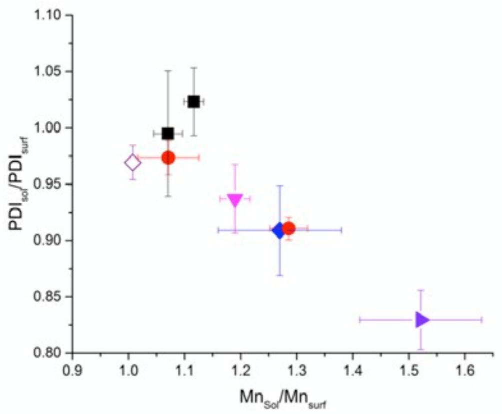

Figure 5. The ratio of PDI in solution to that at the surface against the ratio of molecular weights at in solution and at the surface: ●, ● PMMA, ■, ■ PLMA, ▼ P-t-BMA, ▶ PMA, ◆ PBMA ◇ PS.

1122 L mol^{-1}s^{-1} [21]. Therefore, the low Mn$_{sol}$/ Mn$_{surf}$ may be due to a slow reaction both on the surface and in solution. At lower reaction rates, the influence of crowding at the reaction site will be lower, as more time is available to form the reaction complex between growing polymer, catalyst, deactivator, ligand, and monomer.

Figure 5 shows the ratio of PDI in solution to that at the surface against the Mn$_{sol}$/ Mn$_{surf}$ ratio for all of the polymerizations shown in Figure 1. There is a trend towards decreasing PDI$_{sol}$/PDI$_{surf}$ with increasing Mn$_{sol}$/ Mn$_{surf}$ ratio. That is, as the rate of reaction at the surface becomes slower relative to the rate of polymerization in solution, the PDI at the surface increases relative to the PDI in solution. This is counter-intuitive, as in CRP a slowing of the reaction is generally associated with a decrease in PDI [20, 22]. The deviation from this behavior may thus be attributed to the origin of the decrease in the rate of polymerization, that is, crowding at the reaction site. Patil et al have shown that crowding leads to an increase in termination during surface-initiated polymerization. Thus crowding leads to both a decrease in Mn and an increase in the PDI for surface-grown polymers[9]. Of the monomers investigated in the present study, methyl acrylate is, sterically speaking, the least hindered and thus forms brushes with the highest grafting density, and therefore a higher degree of crowding can be expected at the surface.

Additionally, methyl acrylate has the largest rate coefficient for propagation (k_p) at 33,562 L mol^{-1}s^{-1}, leading to an ATRP reaction rate that is more prone to mass-transfer limitation. At the other extreme, lauryl methacrylate is a bulky monomer with a low grafting density and a relatively low rate coefficient for propagation[23] at 2'870 L mol^{-1}s^{-1}. The crowding at the reactive center, and its effect on the rate of polymerization at the surface will be less than for other monomers, and Mn$_{sol}$/ Mn$_{surf}$ ratios closer to 1 are observed.

Conclusions

The influence of surface grafting on ATRP reaction rate has been examined. Among a series of monomers consisting of alkyl methacrylates and methyl acrylate, it was found that the difference in molecular weight between polymers formed in solution and on surfaces was determined largely by the grafting density of the brushes on the surface. An influence of the rate of propagation was also observed, with a lower rate of propagation giving a lower value of Mn$_{sol}$/Mn$_{surf}$. The influence of both these properties is attributed to crowding at the reaction site during the ATRP process. At high grafting densities and/or high propagation rates, the system is liable to be mass-transfer limited at the surface, and thus it proceeds with a lower overall rate of polymerization compared to that in solution. By lowering grafting density, or dropping the propagation rate at lower temperatures or with less-reactive monomers, the system is less mass-transfer limited, and the polymerization rates in solution and on the surface become more similar.

It was also shown that the PDI$_{sol}$/PDI$_{surf}$ ratio decreases with increasing Mn$_{sol}$/Mn$_{surf}$ This indicates that crowding at the surface not only decreases the rate of reaction relative to that in solution but also increases the probability of chain termination. These findings are consistent with computer-modelling studies performed by Turgman-Cohen et al.[8b, 8c].

In the light of these findings, caution is advised when deducing molecular weights of surface-grafted polymers from those of polymers grown simultaneously in solution. It is essential that the effects of mass-transfer and increased termination probability in the growing grafted polymer chain be taken into account.

Acknowledgements

The authors express their gratitude to Dr. Thomas Schweizer (ETH Zurich, Switzerland) for his help with the SEC measurements. Funding from the ETH Research Commission is gratefully acknowledged.

Notes and references

1 (a) V. Coessens, T. Pintauer and K. Matyjaszewski, *Progress in Polymer Science,* 2001, **26**, 337; (b) J. Pyun, K. and Matyjaszewski, *Chemistry of Materials,* 2001, **13**, 3436; (c) W. A. Braunecker and K. Matyjaszewski, *Progress in Polymer Science.* 2007, **32**, 93; (d) I. Luzinov, S. Minko, V. V. Tsukruk, *Progress in Polymer Science,* 2004, **29**, 635; (e) A. K. Bajpai, S. K. Shukla, S. Bhanu, and S. Kankane, *Progress in Polymer Science,* 2008, **33**, 1088.

2 (a) C. M. Hui, J. Pietrasik, M. Schmitt, C. Mahoney, J. Choi, M. R. Bockstaller, and K. Matyjaszewski, *Chemistry of Materials,* 2014, **26**, 745; (b) M. Ejaz, S. Yamamoto, K. Ohno, Y. Tsujii, and T. Fukuda, *Macromolecules*, 1998, **31,** 5934; (c) S. Edmondson, V. L. Osborne, and W. T. S. Huck, *Chemical Society Reviews.,* 2004, **33**, 14.

3 (a) S. Blomberg, S. Ostberg, E. Harth, A. W. Bosman, B. Van Horn, and C. J. Hawker, *Journal of Polymer Science Part a-Polymer Chemistry,* 2002, **40**, 1309; (b) J. Pyun, S. J. Jia, T. Kowalewski, G. D. Patterson, and K. Matyjaszewski,

Macromolecules. 2003, **36**, 5094; (c) A.-H. Lu, E. L. Salabas, and F. Schueth, *Angewandte Chemie-International Edition.* 2007, **46**, 1222; (d) H. Chirowodza, P. C. Hartmann, and H.Pasch, *Macromolecular Chemistry and Physics,* 2014, **215**, 791.

4 M. Husseman, E. E. Malmstrom, M. McNamara, M. Mate, D. Mecerreyes, D. G. Benoit, J. L. Hedrick, P. Mansky, E. Huang, T. P. Russell, and C. J. Hawker, *Macromolecules,* 1999, **32**, 1424.

5 P. Pasetto, H. Blas, F. Audouin, C. Boissiere, Sanchez, C. M. Save, and B. Charleux, *Macromolecules,* 2009**, 42**, 5983.

6 K. Ohno, T. Morinaga, K. Koh, Y. Tsujii, and T. Fukuda, *Macromolecules*, 2005, **38**, 2137.

7 D. Koylu, and K.Carter, R. *Macromolecules,* 2009**, 42,** 8655.

8 (a) J. Genzer, *Macromolecules*. 2006; **39**, 7157; (b) S. Turgman-Cohen, and J. Genzer, *Macromolecules,* 2010**, 43**, 9567; (c) S. Turgman-Cohen and J. Genzer, *Journal of the American Chemical Society.* 2011**, 133**, 17567.

9 (a) R. R. Patil, S. Turgman-Cohen, J. Srogl, D. Kiserow, J. Genzer, *Langmuir.* 2015**, 31**, 2372; (b) R. R. Patil, S. Turgman-Cohen, J. Srogl, D. Kiserow and J. Genzer, *ACS Macro Letters,* 2015, ***4***, 251.

10 C. Kang, R. M. Crockett, and N. D. Spencer, *Macromolecules,* 2014**, 47**, 269.

11 F. L. McCrackin, E. Passaglia, R. R. Stromberg and H. l. Steinber, *Journal of Research of the National Bureau of Standards Section a-Physics and Chemistry,* 1963**, 67A**, 363.

12 C. P. Holmes, *Journal of Organic Chemistry,* 1997**, 62**, 2370.

13 P. Tao, Y. Li, A. Rungta, , A. Viswanath, J. N. Gao, B. C. Benicewicz, R. W. Siegel, and L. S. Schadler, *Journal of Materials Chemistry,* 2011**, 21**, 18623.

14 P. F. Guo, H.-B. Liu, X. Liu, H.-F. Li, W. Y. Huang and S. J. Xiao, *Journal Physical Chemistry C*, 2010, **114,** 333.

15 S. B. Lee, A. J. Russell and K. Matyjaszewski, *Biomacromolecules,* 2003**, 4,** 1386.

16 K. Matyjaszewski, P. J. Miller, N. Shukla, B. Immaraporn, A. Gelman, B. B. Luokala, T. M. Siclovan, G. Kickelbick, T. Vallant, , H. Hoffmann and T. Pakula, *Macromolecules.* 1999, **32**, 8716.

17 G. Dorman, and G. D. Prestwich, *Trends in Biotechnology,* 2000, **18**, 64.

18 R. Hiorns, *Polymer International*, *4th edition*. 2000, **49,** 2250.

19 Y. Tsujii, K. Ohno, S. Yamamoto, A. Goto and T. Fukuda, *Surface-Initiated Polymerization.* 2006**, 197**, 1.

20 T. E. Patten and K. Matyjaszewski, *Accounts of Chemical Research,* 1999, **32**, 895.

21 S. Beuermann and M. Buback, *Progress in Polymer Science,* 2002. **27,**191.

22 (a) W. Tang, Y. Kwak, W. Braunecker, N. V. Tsarevsky, M. L. Coote and K. Matyjaszewski, *Journal of the American Chemical Society,* 2008, **130**, 10702; (b) W. Tang, and K. Matyjaszewski, *Macromolecules*, 2007, **40**, 1858.

23 W. J. Xu, X. L. Zhu, Z. P. Chen and J. Y. Chen, *Journal of Applied Polymer Science*, 2003; **90**, 1117.

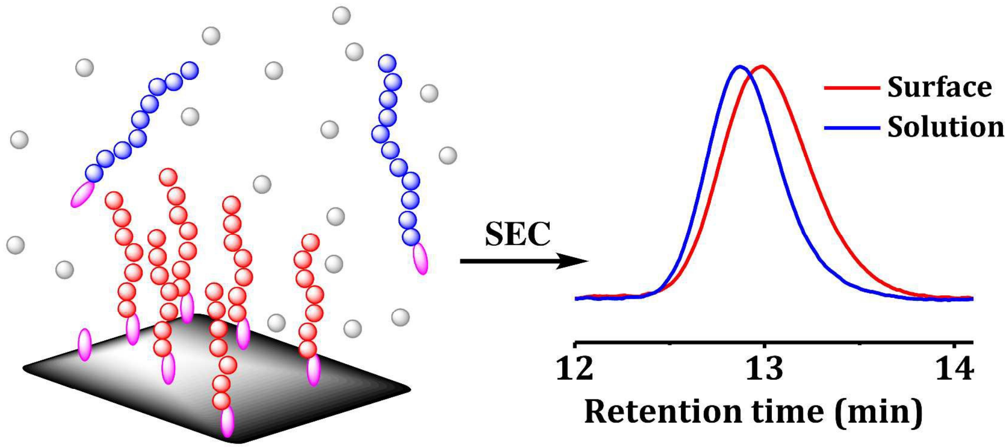

MWs of polymers synthesized simultaneously on a surface and in solution by ATRP differ, depending on the surface grafting density.